

Comparative study on damage identification from Iso-Eigen-Value-Change contours and smeared damage model

N. Lakshmanan¹, B.K. Raghuprasad^{2a}, *N. Gopalakrishnan¹,
R. Sreekala¹ and G.V. Rama Rao¹

¹Structural Engineering Research Centre, CSIR Campus, Taramani, Chennai 600113, India

²Department of Civil Engineering, Indian Institute of Science, Bangalore 560012, India

(Received December 26, 2007, Accepted March 12, 2010)

Abstract. The paper proposes two methodologies for damage identification from measured natural frequencies of a contiguously damaged reinforced concrete beam, idealised with distributed damage model. The first method identifies damage from Iso-Eigen-Value-Change contours, plotted between pairs of different frequencies. The performance of the method is checked for a wide variation of damage positions and extents. The method is also extended to a discrete structure in the form of a five-storied shear building and the simplicity of the method is demonstrated. The second method is through smeared damage model, where the damage is assumed constant for different segments of the beam and the lengths and centres of these segments are the known inputs. First-order perturbation method is used to derive the relevant expressions. Both these methods are based on distributed damage models and have been checked with experimental program on simply supported reinforced concrete beams, subjected to different stages of symmetric and un-symmetric damages. The results of the experiments are encouraging and show that both the methods can be adopted together in a damage identification scenario.

Keywords: damage identification; Iso-eigen-change; smeared damage model.

1. Introduction

The relevant connected papers, which inspire the present work, include that of Morassi (2001), Palacz and Krawczuk (2002), Gladwell's (2004) classical book. The pioneering work and the resulting classical Cawley-Adams criterion states that the ratio of frequency change in two modes is only a function of the damage location and independent of the damage magnitude (Cawley and Adams 1979). The other papers in this field are described subsequently and by no-means the list is exhaustive. A comprehensive survey on damage detection through vibration testing is presented by Doebling *et al.* (1996). Experiments and analytical predictions conducted by Owolobi *et al.* (2003) and Yang *et al.* (2001) provide benchmark data for researchers in this field. Silva and Gomes (1994) have used slotted and fatigue-cracked beams in experimental modal analyses. Cracks in a cantilever

*Corresponding author, Scientist, E-mail: ng@sercm.org

^aProfessor

beam are modeled as a fracture hinge by Ju and Mimovich (1986). Reinforced and plain concrete beams are tested by Choudhury and Ramirez (1992) where changes in resonant frequencies and power spectral densities of displacements resulting from simulated damage are studied. Polycarbonate cantilever beam having an opening and closing crack in the interior of the beam, running parallel to the top and bottom surfaces is studied by Prime and Shevitz (1996). Lakshmanan *et al.* (1991) and Rajagopalan *et al.* (1996, 1999) have correlated the cracking and yielding stiffness of the normal and fiber-reinforced concrete beams, under various stages of pre-loading with the fundamental frequencies. A method is outlined such that from frequency measurements, maximum load carried by the bridge in its life time could be estimated. Hassiotis and Jeong (1993) and Hassiotis (2000) outlined a method based on first order perturbation and optimization theory to compute the damage from measured natural frequencies. Recently, wavelet based damage detection technique, which makes use of dynamic and static response and using ANN techniques are dealt with by Lakshmanan *et al.* (2007a, b, 2008a, b).

Damage identification using measured natural frequencies, with the damage modelled as an equivalent rotational spring is dealt with by Liang *et al.* (1992), Nandwana and Maiti (1997) and Patil and Maiti (2003). Anti-resonant frequency based damage identification is proposed by Dilena and Morassi (2004, 2009). Casas and Aparicio (1994) advocate a higher mode based damage identification methodology using dynamic test data. Cerri and Vestroni (2000, 2005) deal with distributed damage model and uses pseudo-experimental values to validate their method. They have employed a minimisation procedure based on output error to identify damage in a reinforced concrete element. In a recent paper Morassi (2007) proposes a damage identification methodology using Fourier coefficients. Non-linear vibration characteristics and amplitude based damping values are used as tools for damage identification by Neild *et al.* (2003).

2. Distributed damage model

In this model, applicable for a damaged reinforced concrete structure, each damaged element has a reduced $(EI)_{eff}$, depending upon the moment, axial and shear force. Typically the moment curvature ($M-\phi$) relationship of a reinforced concrete structural member, dominated by flexure could be estimated, using a fibre theory. The neutral axis depth is sequentially progressed with varying concrete strains at extreme fibre, such that force equilibrium is achieved. The moment-curvature pair, giving rise to such an equilibrium state could then be estimated. This can also be calculated using reasonably valid approximated expressions, using a tri-linear ($M-\phi$) relationship, denoting the transition between cracking, yielding and ultimate moment stages. The effect of axial force could also be accounted in estimating such relationships. The slope of the moment curvature curve could then be used to estimate $(EI)_{eff}$ at a particular section depending on the moment carried by that section. A quasi-brittle material like concrete, combined with reinforcing steel and having a large number of closely spaced cracks, under conditions of high bond stress between steel and concrete could be conveniently represented by an $(EI)_{eff}$ model, both for calculating deflections and also for computing the natural frequencies of a flexure-dominated beam.

The parameters that define a damage are shown in Fig. 1, for a contiguous single distributed damage, position of damage given by, l_0/l , extent of damage as, $2b_0/l$ and the magnitude of damage as, β . All these parameters are thus non-dimensionalised.

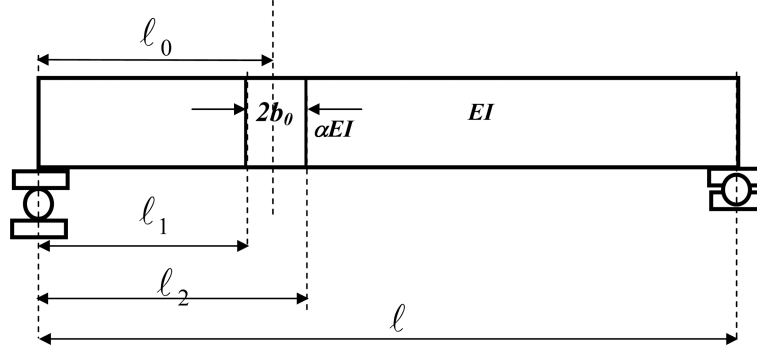


Fig. 1 Simply supported beam with a reduced EI for portion of its length

2.1 Natural frequency change as a perturbation problem (Gatti and Ferrari 1999)

A perturbation analysis of the non-degenerate dynamic system with small perturbations occurring in its stiffness and mass matrices is made use of to derive appropriate equations.

The unperturbed (zeroth-order) problem is

$$K_0 p_i^{(0)} = \lambda_i^{(0)} M_0 p_i^{(0)} \quad (1)$$

\mathbf{K}_0 and \mathbf{M}_0 are the stiffness and mass matrices at the initial state and $\lambda_i^{(0)}$ and $\mathbf{p}_i^{(0)}$ are the corresponding i -th eigen value and vector. If \mathbf{K}_1 and \mathbf{M}_1 be the small perturbations in stiffness and mass matrices respectively, then the perturbed problem could be written as

$$(\mathbf{K}_0 + \mathbf{K}_1) p_i = \lambda_i (\mathbf{M}_0 + \mathbf{M}_1) p_i \quad (2)$$

The eigenvalues and vectors can be expanded in terms of a parameter γ , such that zeroth, first, etc., powers of γ correspond to the zeroth, first orders of perturbation analysis. The perturbed portion of the original matrix, namely \mathbf{K}_1 and \mathbf{M}_1 can be replaced by $\gamma \cdot \mathbf{K}_1$ and $\gamma \cdot \mathbf{M}_1$ and λ_i and \mathbf{p}_i are expressed as power series in γ .

The perturbed eigenvalues and vectors are written as

$$\begin{aligned} \lambda_i &= \lambda_i^{(0)} + \gamma \cdot \lambda_i^{(1)} + \gamma^2 \cdot \lambda_i^{(2)} + \dots \\ p_i &= p_i^{(0)} + \gamma \cdot p_i^{(1)} + \gamma^2 \cdot p_i^{(2)} + \dots \end{aligned} \quad (3)$$

By substituting the perturbed eigenvalues and vectors into Eq. (6), one obtains the following modified eigenvalue problem

$$\begin{aligned} (\mathbf{K}_0 + \gamma \cdot \mathbf{K}_1)(p_i^{(0)} + \gamma \cdot p_i^{(1)} + \gamma^2 \cdot p_i^{(2)} + \dots) &= (\lambda_i^{(0)} + \gamma \cdot \lambda_i^{(1)} + \gamma^2 \cdot \lambda_i^{(2)} + \dots) \\ (\mathbf{M}_0 + \gamma \cdot \mathbf{M}_1)(p_i^{(0)} + \gamma \cdot p_i^{(1)} + \gamma^2 \cdot p_i^{(2)} + \dots) & \end{aligned} \quad (4)$$

After equating coefficients of equal powers of γ on both sides of the equation, we can write the zeroth, first and higher order perturbation equations. These are

$$\begin{aligned}
 K_0 p_i^{(0)} &= \lambda_i^{(0)} M_0 p_i^{(0)} \\
 K_0 p_i^{(1)} + K_1 p_i^{(0)} &= \lambda_i^{(0)} M_0 p_i^{(0)} + \lambda_i^{(0)} M_1 p_i^{(0)} + \lambda_i^{(1)} M_0 p_i^{(0)}
 \end{aligned}
 \tag{5}$$

It is seen that zeroth order problem is the unperturbed problem. The vector $\mathbf{p}_i^{(1)}$ can be expanded on the basis of unperturbed eigen vectors and may be written as

$$p_i^{(1)} = \sum_r c_{ir} p_r^{(0)}
 \tag{6}$$

The scalar c_{ir} is the scaling factor, with which the original mode shapes are modified to render perturbed mode shapes. After simplification and imposing ortho-normalizing properties for both old and new eigen vectors, the first order perturbation calculations of i -th eigenvalues and vectors can be written as

$$\begin{aligned}
 \lambda_i &= \lambda_i^{(0)} + p_i^{(0)T} (K_1 - \lambda_i^{(0)} M_1) p_i^{(0)} \\
 p_i &= p_i^{(0)} - \left(\frac{1}{2} p_i^{(0)T} M_1 p_i^{(0)} \right) \cdot p_i^{(0)} + \sum_{\substack{r=1 \\ r \neq i}}^n \left(\frac{p_r^{(0)T} (K_1 - \lambda_i^{(0)} M_1) p_i^{(0)}}{\lambda_i^{(0)} - \lambda_r^{(0)}} \right) \cdot p_r^{(0)}
 \end{aligned}
 \tag{7}$$

For the condition of a damaged structure, wherein the mass matrix does not undergo any change from the original matrix, the above equation can be further simplified as

$$\begin{aligned}
 \lambda_i &= \lambda_i^{(0)} + p_i^{(0)T} K_1 p_i^{(0)} \\
 p_i &= p_i^{(0)} + \sum_{\substack{r=1 \\ r \neq i}}^n \left(\frac{p_r^{(0)T} K_1 p_i^{(0)}}{\lambda_i^{(0)} - \lambda_r^{(0)}} \right) \cdot p_r^{(0)}
 \end{aligned}
 \tag{8}$$

From Eq. (8), it can be noted that only the i th un-perturbed eigen parameters enter into the calculations of perturbed eigenvalues, whereas the complete unperturbed eigen solution is required for the computation of the perturbed eigenvectors.

The perturbation equation states that the new values of frequencies can be obtained by using the original unperturbed eigen functions.

$$\omega_d^2 = \frac{\int_0^{\ell_0 - b_0} EI \cdot \left(\frac{d^2 y}{dx^2} \right)^2 dx + \int_{\ell_0 - b_0}^{\ell_0 + b_0} \alpha EI \cdot \left(\frac{d^2 y}{dx^2} \right)^2 dx + \int_{\ell_0 + b_0}^{\ell} EI \cdot \left(\frac{d^2 y}{dx^2} \right)^2 dx}{\int_0^{\ell} \overline{m} y^2 dx}
 \tag{9}$$

where $y_n(x) = \sin(n\pi x/\ell)$ is the mode shape corresponding to the initial state. By making a substitution of $\beta = 1 - \alpha, 0 \leq \alpha \leq 1$, (where α is the ratio of the damaged EI as compared to the original EI and β is the magnitude of damage) in the previous equation and simplifying, the following expression for the normalized natural frequency is obtained for the damaged simply supported beam.

$$\left(\frac{\omega_d}{\omega}\right)_n = \sqrt{1 - 2\beta \left[\frac{b_0}{\ell} - \frac{1}{2n\pi} \left(\cos \frac{2n\pi\ell_0}{\ell} \cdot \sin \frac{2n\pi b_0}{\ell} \right) \right]} \quad (10a)$$

$$\left(\frac{\Delta\omega^2}{\omega^2}\right)_n = 2\beta \left[\frac{b_0}{\ell} - \frac{1}{2n\pi} \left(\cos \frac{2n\pi\ell_0}{\ell} \cdot \sin \frac{2n\pi b_0}{\ell} \right) \right] \quad (10b)$$

For the case of a beam with a uniform reduction of EI to αEI for its entire length, the equation reduces to a simplest case possible

$$\left(\frac{\omega_d}{\omega}\right)_n = \sqrt{1 - \beta} = \sqrt{\alpha} \quad (11)$$

If further simplifications are made in the foregoing equation for the case of a crack situated at the centre and for values of b_0 tending towards zero

$$\left(1 - \left(\frac{\omega_d}{\omega}\right)^2\right)_n \cong \frac{2\beta \cdot b_0}{\ell} [1 - (-1)^n] \quad (12)$$

Eq. (12) states that for a centrally situated defect, with length closer to zero, even-numbered modes have no reduction in their frequencies. The above set of equations, though approximate and simple and based on a first order perturbation theory, sheds insights into some concepts as summarized below.

(a) The defect in a beam manifested in the form of a reduction in its fundamental frequencies is a function of (i) position of damage l_0 , (ii) extent of damage $2b_0$ and (iii) the magnitude of damage β .

(b) The position of damage is such that it is sensitive to certain set of frequencies only. The simple example is the invariance of even numbered modes to a centrally situated damage.

(c) The upper-bound of the reduced frequency for a magnitude of damage β is at best $\sqrt{\beta}$, when the reduction in EI is full and widespread. In all other cases it is less than this value. However for a total uniform reduction in EI , the mode shape does not change from the original state.

2.2 Damage identification from Iso-Eigen-Value-Change contours and case studies (Lakshmanan et al. 2010)

Ratio of the changes in Eigen values are obtained after modifying and re-writing Eq. (10b) as

$$\frac{\Delta\omega_n^2/\omega_m^2}{\Delta\omega_m^2/\omega_n^2} = \frac{\Delta\omega_n^2 m^4}{\Delta\omega_m^2 n^4} = \frac{\left[\frac{b_0}{\ell} - \frac{1}{2n\pi} \left(\cos \frac{2n\pi\ell_0}{\ell} \cdot \sin \frac{2n\pi b_0}{\ell} \right) \right]}{\left[\frac{b_0}{\ell} - \frac{1}{2m\pi} \left(\cos \frac{2m\pi\ell_0}{\ell} \cdot \sin \frac{2m\pi b_0}{\ell} \right) \right]} \quad (13)$$

It is thus proved that the ratio of changes in Eigen values (squared frequencies) are independent of the magnitude of damage and are functions of only the central position of damage and its extent. Indirectly, the method is to find out the ratio of variation in frequencies as the normalising factor, ω_m^2/ω_n^2 , is only m^4/n^4 , which is a constant for any pair of frequencies. Having eliminated a variable (β), out of three, it is possible to construct curves such that the variation of Eigen-change-ratios can be visualised. Varying values of $2b_0/\ell$, ℓ_0/ℓ which give rise to constant Eigen-change-ratios $\Delta\omega_n^2/\Delta\omega_m^2 \cdot \omega_m^2/\omega_n^2$, for a simply supported beam are plotted in the form of contours. Figs. 2 and 3 show the contours of equal Eigen-change-ratios, for pairs of Eigen values namely 2-1 ($n=2$, $m=1$)

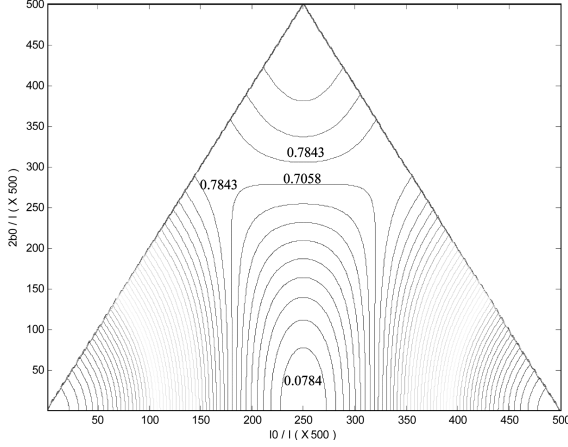


Fig. 2 Iso-Eigen-Change contours for frequency ratio 2 : 1 (Increment : 0.07843)

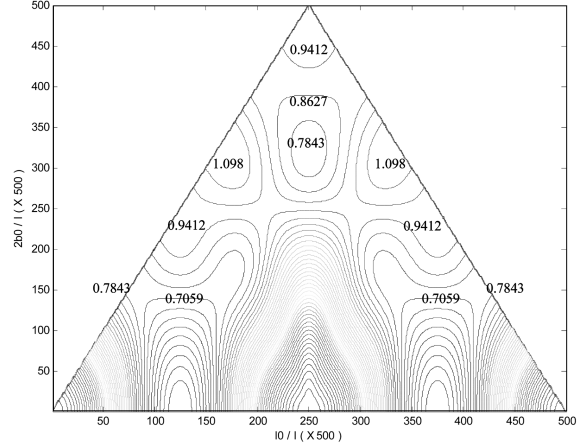


Fig. 3 Iso-Eigen-Change contours for frequency ratio 4 : 2 (Increment : 0.07843)

and 4-2, respectively. The curves are generated for a beam of 500 segments.

The exercise is not just a theoretical one and certain physical in-sights are obtained:

(a) Contours are symmetrical indicating that a symmetrical damage affects the frequencies equally.
 (b) The $\pi/4$ radians boundary line shows that the extent of damage $2b_0/l$, on the Y-axis shall at best be twice the centre of damage location l_0/l , on the X-axis.

(c) Contours at the top most point of the figure, indicate a wide-spread constant damage and all frequencies are affected equally and hence the ratio is 1.0.

(d) Contours closer to support are around 3 to 4, indicating that high frequencies are affected more by off-centric damage.

(e) As a converse of point (d), contours closer to mid-span, for 21, 31 and 41 contours show smaller values especially for small amounts of damage.

This exercise on the theoretical damage identification study involves certain example problems which are solved using these contours.

The six example validation problems (Lakshmanan *et al.* 2010) solved are as follows : (β is the magnitude of damage, kept as 0.10)

$$(a) \frac{2b_0}{l} = 0.1, \frac{l_0}{l} = 0.25, \beta = 0.1$$

$$(b) \frac{2b_0}{l} = 0.3, \frac{l_0}{l} = 0.25, \beta = 0.1$$

$$(c) \frac{2b_0}{l} = 0.10, \frac{l_0}{l} = 0.144, \beta = 0.1$$

$$(d) \frac{2b_0}{l} = 0.20, \frac{l_0}{l} = 0.144, \beta = 0.1$$

$$(e) \frac{2b_0}{l} = 0.30, \frac{l_0}{l} = 0.5, \beta = 0.1$$

$$(e) \frac{2b_0}{l} = 0.20, \frac{l_0}{l} = 0.5, \beta = 0.1$$

It is seen than case (a) to case (d) are un-symmetrical damage patterns and case (e) and case (f) are symmetrical damages. For example, in case (a) $\Delta\omega_n^2/\Delta\omega_m^2$ ω_m^2/ω_n^2 for the pairs of 2-1, 4-2, 3-1 and 4-1 frequency ratios are 1.897, 0.129, 0.968 and 0.245 respectively. The intersection point of all the contours indicate the position and extent of damage, which in this case works out to be 0.25 and 0.1 respectively (Fig. 4(a)). Figs. 4(b) shows the results of case (b). After the geometric details of

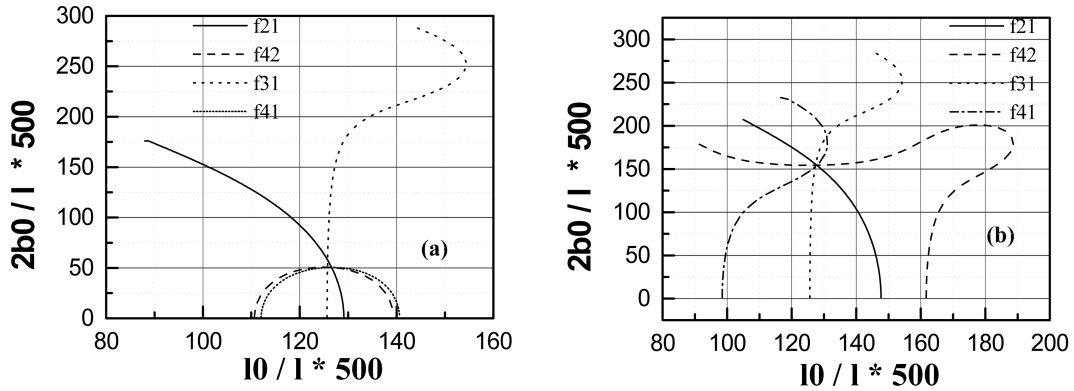


Fig. 4 (a,b) Prediction of damage position and extent from Iso-Eigen-change contours (a) D1, (b) D2

the damage are got, Eq. (10b) is used to extract the magnitude of damage. The least square estimation can be adopted, for this over-determined set of equations, (with four equations and one un-known), which in this case works out to be 0.10.

It is to be observed that, for symmetrical damages, the intersection point is also a point of zero slope and hence the contours are tangential to each other. An extra frequency information may be required to resolve this issue or additionally, the authors (Lakshmanan *et al.* 2008b) propose a static based system identification procedure, which shall resolve a symmetric and an un-symmetric damage, in conjunction with dynamic measurements.

2.3 Effect of error bounds on Iso-Eigen-Value-Change contours

An extension of this work is the study of the performance of this damage identification methodology, with errors in frequency ratios. The previously mentioned case studies, namely, (a) $2b_0/l = 0.1, l_0/l = 0.25, \beta = 0.1$ (b) $2b_0/l = 0.3, l_0/l = 0.25, \beta = 0.1$ are repeated with error bounds in measurements (Lakshmanan *et al.* 2010). For example, an error bound of $\pm 5\%$ is

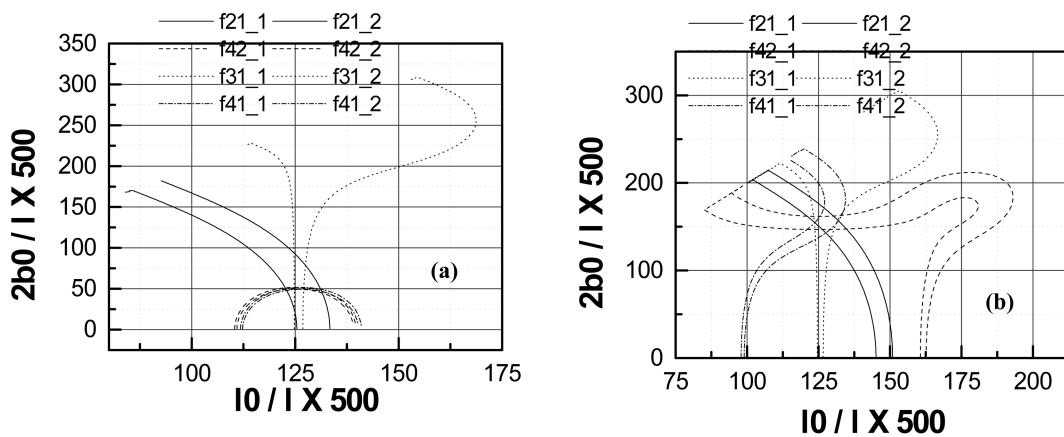


Fig. 5 Prediction of damage position and extent with 5% error bounds from Iso-Eigen-change contours (a) D1, (b) D2

introduced artificially on each of these contour plots. This means that the previously generated contours, would have given rise to a fresh pair of contours of values 0.95 and 1.05 times the original values. All the eight curves are super-imposed and shown for these two cases (Fig. 5(a) and Fig. 5(b)). The inference is that, even though the region of intersection has widened, divergence of results is not seen and the centre of the intersected area is still the actual damaged point. Also it is to be noted that errors of 5% magnitudes are rather large. Ideally typical source or error is the change in the frequency, for a small extent of damage situated in a node position of a beam, thus giving a small change in $\Delta\omega^2$. This coupled with the frequency resolution in FFT, may end up giving a larger error.

2.4 Application of Cawley-Adams criterion for a discrete structure with a contiguous single damage

The method of Cawley-Adams criterion and the resulting equations are used to identify a single uniform damage for a simply supported beam in the previous section. However, for a discrete structure, a general purpose closed form expression may not be easily derived and a numerical exercise is carried out to generate the frequency shift information for a five storied, three-bay shear frame (Fig. 6). The damage is assumed as contiguous. Five cases are computationally evaluated, namely, single storey damage, two contiguous storey damage, three contiguous storey damage and up to all five storey damage. The centre of damage is also varied from the bottom most storey to the top storey. The information on the ratio of Eigen value shift between various modes are evaluated and plotted. Fig. 7 shows the ratio of Eigen-value change between (a) second and first modes and (b) between third and first modes. Fig. 8 shows the ratio of Eigen-value change between (a) third and second modes and (b) between fourth and first modes. X-axis shows the position of damage and Y-axis gives the ratio of Eigen value change. These curves, though generated for a $\beta = 10\%$ are valid for larger values of β up to 30%.

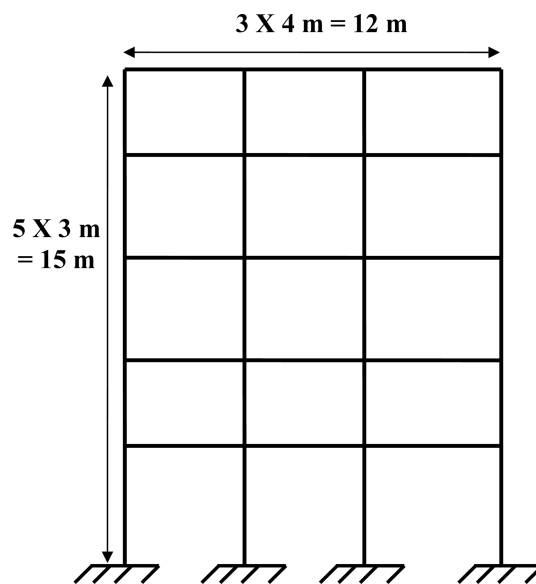


Fig. 6 Discrete structure taken for damage estimation using Cawley-Adam's criterion

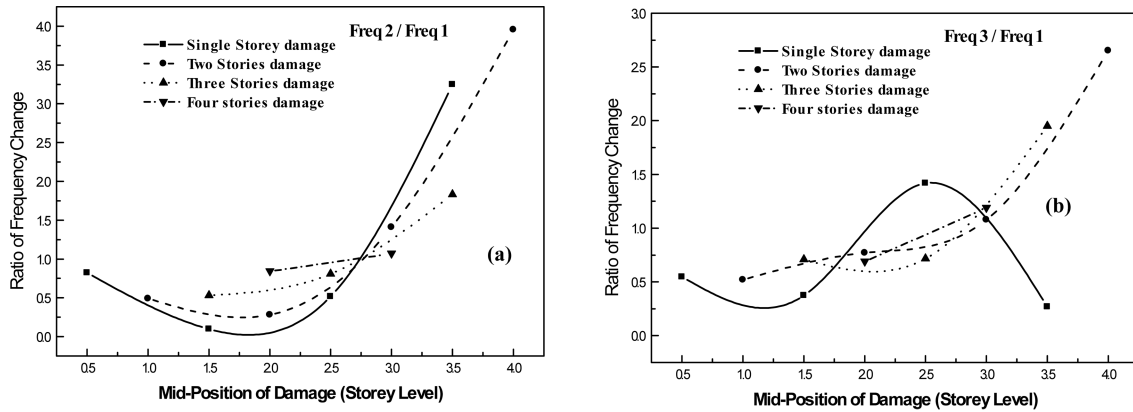


Fig. 7 Ratio of Eigen value change for the discrete structure between (a) second and first and (b) third and first modes

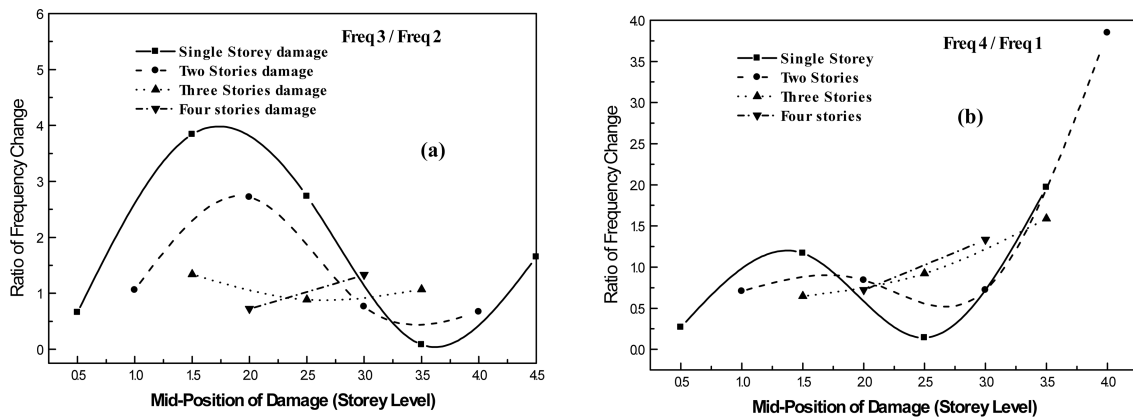


Fig. 8 Ratio of Eigen value change for the discrete structure between (a) third and second and (b) fourth and first modes

Let us see as to how these set of curves could be used to find the damage of this framed structure. A uniform damage of bottom three storeys is assumed to be inflicted on to this structure, as a result of which the first five frequencies have undergone a change. The following data is obtained as a result of experimental modal analysis on this shear structure prior to and after damage:

- (a) Eigen values prior to damage : 8.1014, 69.0279, 171.5370, 283.0830, 368.2507
- (b) Eigen values after damage : 7.3903, 65.8189, 160.8715, 267.0006, 348.9188
- (c) Ratio of Eigen value Change : 0.08775, 0.04648, 0.06218, 0.05681, 0.05250
- (d) Ratio of change in Eigen values between modes : 0.53 (Second to first mode), 0.71 (Third to first mode), 1.34 (Third to second modes), 0.65 (Fourth to first mode)

From inspection of Figs. 7 and 8, the following damage possibilities exist:

Second to first mode:

- (a) Bottom three storeys
- (b) Single storey at third floor

Third to first mode:

- (a) Bottom three storeys
- (b) Middle 3 storeys

Third to Second mode:

- (a) Bottom three storeys
- (b) Top four storeys
- (c) Top three storeys

Fourth to first mode:

- (a) Bottom three storeys
- (b) Bottom two storeys
- (c) Third and fourth storeys

Out of these various possibilities, we may conclude that the only possibility that is common for all Eigen value changes is : Damage to bottom three storeys. Thus we can say the Cawley-Adams criteria hold promise for damage identification even for a discrete structure.

2.5 Evaluation of extent of damage for a symmetric damage

We shall try to resolve the problems in identification of symmetrical central damage for a simply supported beam from the Iso-Eigen-Value-Change contours by resorting to another related method. Supposing that an a-priori knowledge exists such that the likely damage onto a structure is symmetric, distributed and centrally located, the fact is advantageously utilised to estimate both the extent of damage and the magnitude. We shall revert back to Eq. (10b) and simplify the same for symmetric damages.

$$\left(\frac{\Delta\omega^2}{\omega^2}\right)_n = \frac{2\beta \cdot b_0}{\ell} \left[1 - \frac{\ell}{2n\pi b_0} (-1)^n \sin \frac{2n\pi b_0}{\ell} \right] \tag{14a}$$

$$\left(\frac{\Delta\omega^2}{\omega^2}\right)_n = \frac{2\beta \cdot b_0}{\ell} [1 - (-1)^n \text{sinc}(n\pi x)]; \quad x = \frac{2b_0}{\ell} \tag{14b}$$

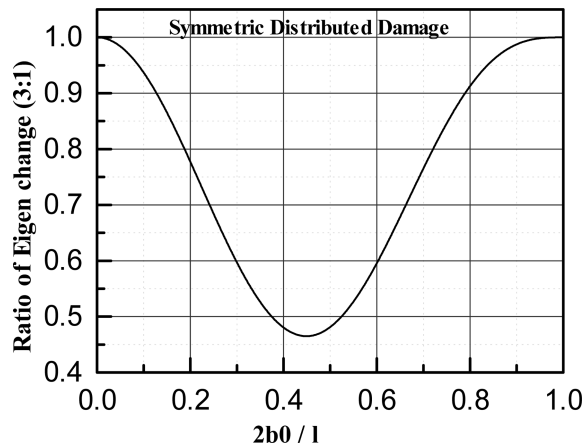


Fig. 9 Prediction of damage extent for a symmetrical distributed damage with Eigen-value-change-ratio between third and first modes

$$\frac{\Delta\omega_n^2 \cdot \omega_m^2}{\omega_n^2 \cdot \Delta\omega_m^2} = \frac{1 - (-1)^n \text{sinc}(n\pi x)}{1 - (-1)^m \text{sinc}(m\pi x)} \quad (14c)$$

Between the third and first modes, the equation is further simplified as

$$\frac{\Delta\omega_3^2}{81\Delta\omega_1^2} = \frac{1 + \text{sinc}(3\pi x)}{1 + \text{sinc}(\pi x)} \quad (14d)$$

Eq. (14d) is plotted in Fig. 9 and the horizontal intersection point on this bell-shaped curve for an Eigen-change-ratio obtained from the experiment shall indicate the extent of uniform damage. However, there are two points of intersection, which can be resolved by solving Eq. (14a), for both the points and estimating the true extent of damage and its magnitude. The previous cases (e) and (f), which have given a ratio of 0.58 and 0.76 are solved and the damage extent is estimated as 30% and 20% respectively.

2.6 Smearred distributed damage model

For a multiple damage scenario, Eq. (10) is modified and written as

$$1 - \left(\frac{\omega_d}{\omega}\right)_n^2 = \sum \beta_j \left[\frac{2b_{0,j}}{\ell} - \frac{1}{n \cdot \pi} \left(\cos \frac{2n \cdot \pi \cdot \ell_{0,j}}{\ell} \cdot \sin \frac{2n \cdot \pi \cdot b_{0,j}}{\ell} \right) \right] \quad (15)$$

In Eq. (15), β_j is the reduction in EI at the ' j -th' segment and the damage exists for a length of $b_{0,j}$ and the distance to the mid-point of this segment is $\ell_{0,j}$. Such an equation can be written for each measured frequency and there will be n equations corresponding to n measured sets of frequencies. Eq. (15) can be written in a matrix form in the following manner and the information of damage could then be obtained for as many locations as the number of measured frequencies.

$$\{\varepsilon\} = [A]\{\beta\} \quad (16a)$$

$$\varepsilon_i = 1 - \left(\frac{\omega_d}{\omega}\right)_i^2$$

$$A_{ij} = \frac{2b_{0,j}}{\ell} - \frac{1}{i\pi} \left(\cos \frac{2i\pi\ell_{0,j}}{\ell} \cdot \sin \frac{2i\pi b_{0,j}}{\ell} \right) \quad (16b)$$

where, the subscript i is the variation for the number of measured modes and the subscript j is the variation of number of beam segments. The essential pre-requisite for this model is that lengths and positions of damaged segments have to be given as initial input. And the matrix in Eq. (16a) is solved either normally or in a least square sense. Towards verifying the above procedure, a numerical exercise is carried out for a simply supported beam, in which damage is introduced in the form of reduced EI at ten equal segments (0.1ℓ). Natural frequencies for the first five modes are computed during the undamaged state of the beam and after inducing damage. This gives rise to the left hand side of Eq. (16a), where the ratio of the change in the Eigen values after occurrence of damage to the original Eigen value is to be given. The matrix $[A]$ is a function of the length and mid-positions of segments. Using the information and making use of symmetry, total numbers of unknowns are five and hence five equations are needed for solution. A computer program is written,

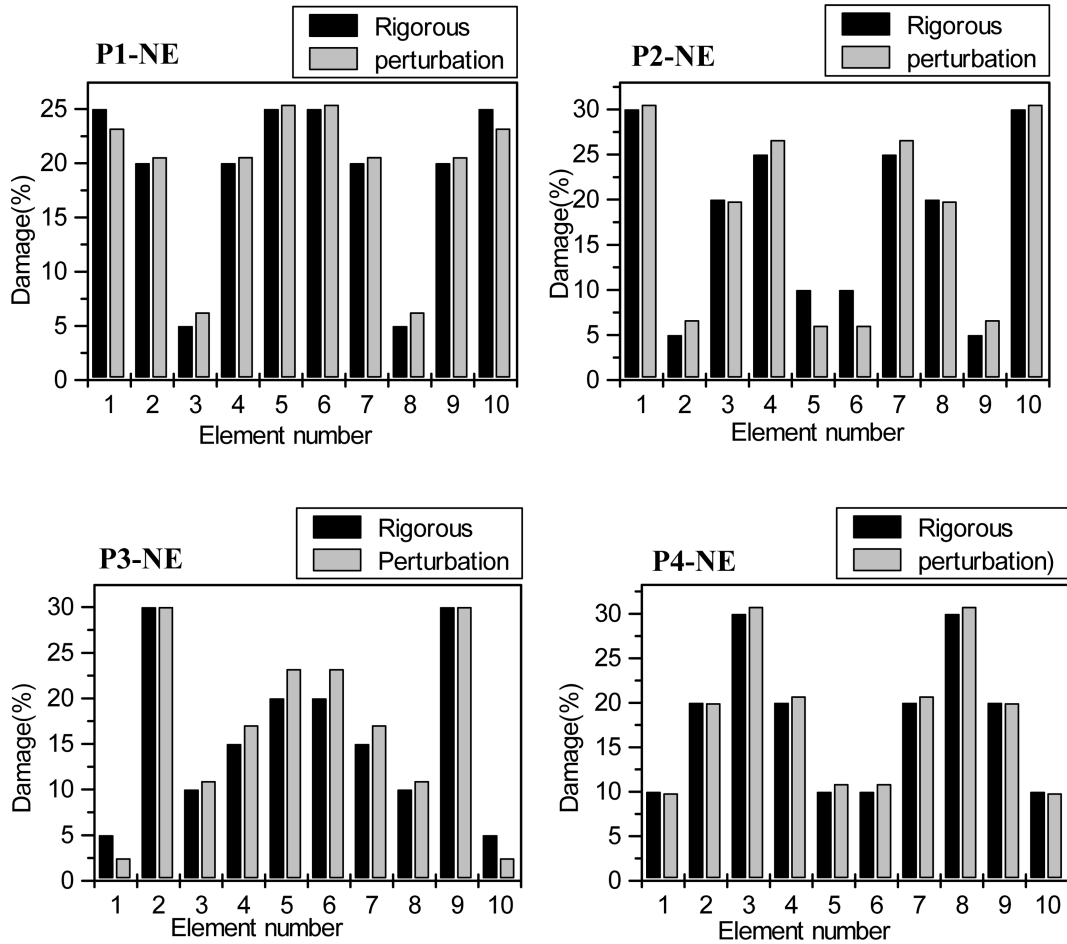


Fig. 10 Comparison of damage magnitudes predicted by smeared damage model with simulated damage values (Damage pattern : P1-NE to P4-NE)

which takes the frequencies of the beam prior to and after damage. Using this input, the program computes the damage on each of the beam segment. The damage distribution is assumed to be symmetric. Physically in the case of a bridge, suffering damage due to traffic induced loading, bending moment and shear force distributions are symmetrical and hence a symmetrical damage pattern can be reasonably assumed. Also, such an assumption gives rise to information on damage at '2N' sites, if frequency information is available only for 'N' modes. However, in cases where the damage is really un-symmetric, then some additional assumptions have to be made on the extent of the damage and this also has to be kept un-symmetric to solve Eq. (16). The resulting matrix becomes singular, for a symmetric distribution of the extent of damage, if the condition of symmetry is not explicitly made use of.

Figs. 10 and 11 compare the damages predicted by the method vis-à-vis the actual damages. As can be seen from these figures, a wide variation of damage patterns are simulated and tested to evaluate the efficiency of the developed method. It is important to verify the range of validity of

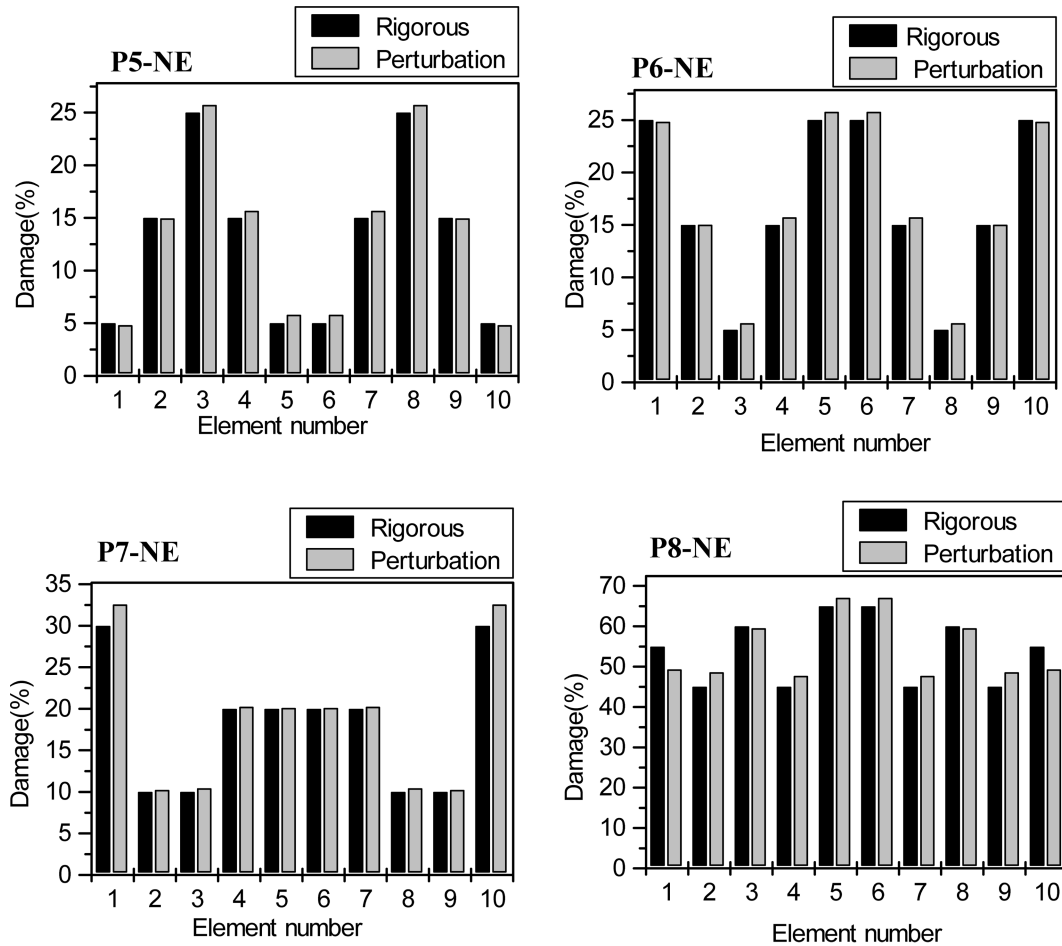


Fig. 11 Comparison of damage magnitude predicted by smeared damage model with simulated damage values (Damage pattern : P5-NE to P8-NE)

Eqs. (15), (16a) and (16b), as the first-order perturbation method (or Eigen sensitivity method) is approximate. Also, damage identification algorithms are known to produce false-alarms at undamaged zones, particularly when the region is of relatively low strain energy density. For example, it is easier to detect damage at a simply supported beam-centre or a cantilever beam-support, due to the higher contribution of the elements situated at these places towards frequency reduction. Hence a large damage has to be simulated at supports and tested. Further, wherever, the damage pattern cannot be described as smooth Fourier functions and there are abrupt variations, then also the detection algorithm may show errors. Hence the testing cases involve,

- Progressively increasing damage magnitudes
- Damage patterns following typical mode shape patterns
- Damage patterns following the reversed mode shape patterns $(1 - \sin(n\pi x/\ell))$
- Abrupt variation of damages in adjacent elements.

Table 1(a) Comparison of simulated and retrieved damages (%) (P1-NE to P6-NE)

Beam Segment	P1-NE		P2-NE		P3-NE		P4-NE		P5-NE		P6-NE	
	S ⁺	R ⁺⁺										
1	25	23.2	30	30.5	5	3.0	10	9.8	5	4.8	25	24.8
2	20	20.5	5	6.6	30	30.0	20	20.0	15	14.9	15	15.0
3	5	6.2	20	19.8	10	11.0	30	30.8	25	25.7	5	5.6
4	20	20.6	25	26.6	15	17.0	20	20.7	15	15.7	15	15.7
5	25	25.4	10	7.0	20	23.2	10	10.9	5	5.8	25	25.8

Table 1(b) Comparison of simulated and retrieved damages (%) (P7-NE to P12-NE)

Beam Segment	P7-NE		P8-NE		P9-NE		P10-NE		P11-NE		P12-NE	
	S ⁺	R ⁺⁺										
1	30	32.6	55	49.3	70	72.2	70	68.1	20	26.7	70	89.8
2	10	10.2	45	48.6	65	63.2	65	68.3	50	50.9	40	38.7
3	10	10.5	60	59.5	60	63.4	75	75.9	30	32.4	60	64.1
4	20	20.3	45	47.7	75	76.4	85	81.3	50	51.0	30	35.5
5	20	20.1	65	67.1	75	75.3	85	86.4	40	40.1	40	39.7

S⁺ : Simulated damage % ; R⁺⁺ : Retrieved damage %

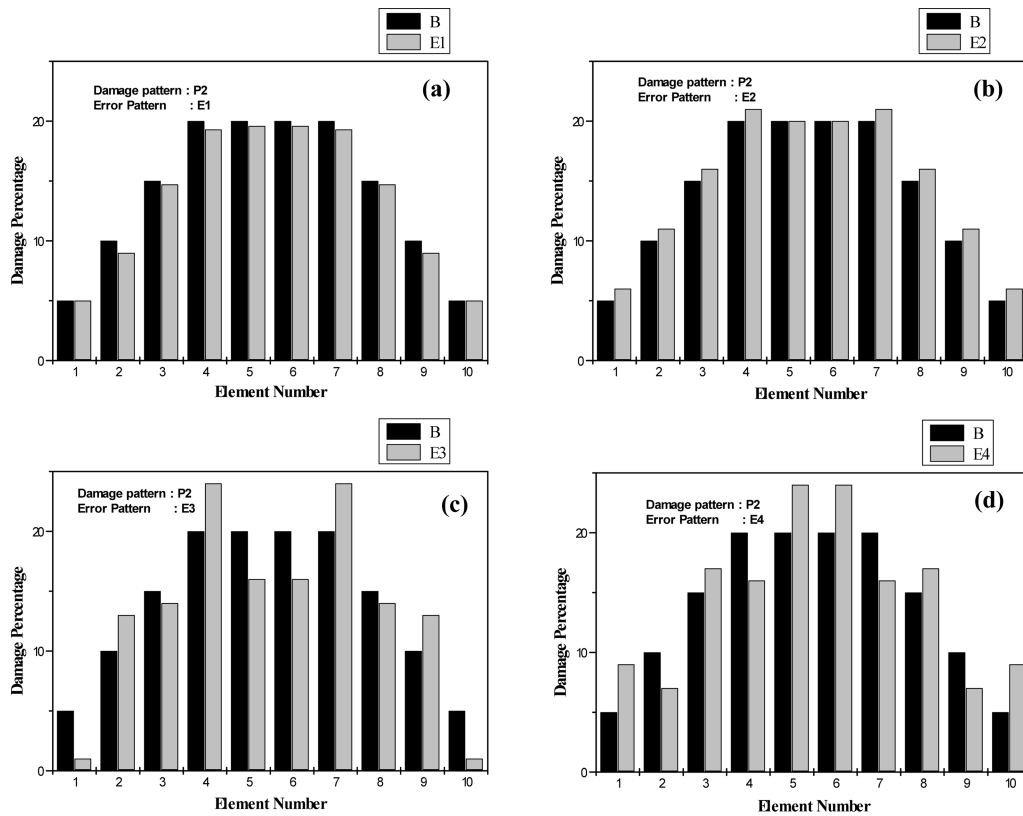


Fig. 12 Performance of smeared damage model (Damage pattern : P2) with artificial error ingress (a) error pattern E1 (b) error pattern E2 (c) error pattern E3 (d) error pattern E4

Tables 1(a) and 1(b) show the various patterns (P1-NE to P12-NE, NE stands for no measurement errors) as validation examples giving a comparison of simulated and retrieved damages. Damages in beam segments 6-10 are symmetric with reference to centre line of the beam (Beam segment-1 is near support and 5 is near mid-span). Towards verification of the performance of the method in the presence of noise an artificial noise ingress in the form of (a) uniform +1% distortion, (b) uniform -1% distortion and (c and d) flip-flop 1% error is induced and the retrieved damages are plotted in Fig. 12.

The following trends can be observed regarding the inverse problem of damage retrieval from changes in Natural frequencies (Figs. 10, 11 and 12 and Tables 1(a) and 1(b)):

- (a) Up to 30% damage values, the prediction is within tolerable limits.
- (b) Difference in the predicted value is more at regions of less strain energy density.
- (c) The method predicts damages well, even when its variation is abrupt and not smooth.
- (d) For larger damage values (more than 30%), the prediction is good if the average damage is not very much different from the peak damage. Where there is larger variation between damages, the prediction shows higher errors.
- (e) The percentage difference is the maximum at regions of lower damage values.

2.7 Comparison of smeared damage model with the method of Iso-Eigen-Value-Change contours

Table 2 gives the comparative evaluation of both the methods and also lists the pros and cons of each method.

2.8 Experimental investigations

There are two algorithms discussed, one based on Iso-Eigen-Value-Change contours for uniform distributed damage and the other is a smeared damage model with the necessary inputs on the lengths and positions of the segments. Iso-Eigen-Value-Change contours lend themselves to simple curves if a-priori information on the symmetrical damage is available. Laboratory testing is carried on four reinforced concrete beams with simply supported boundary conditions. These beams are

Table 2 Comparison of the two methods

Aspect compared	Smeared damage model	Iso-Eigen-Value-Change contours
Method of damage detection	Natural frequency based ; requires change in frequency ratio.	Natural frequency based; requires ratio of change in frequencies between two modes.
Multiple/single damage identification	Multiple damage and uniform damage within a segment	Single contiguous and uniform damage
Limitation of Damage magnitude	Found to be valid up to 30% damage	Since damage magnitude is not explicitly used, valid for larger magnitudes of damage
Limitation	Requires initial input on position and extent of damage	Estimates position and extent but magnitude has to be still estimated by smeared damage model

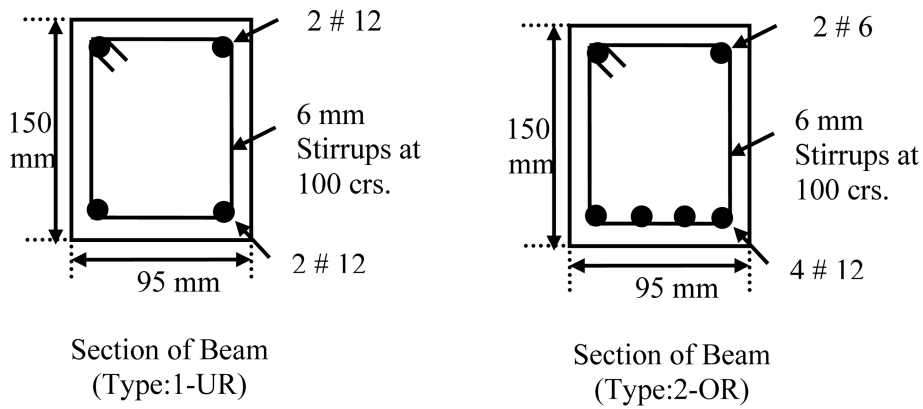


Fig. 13 Section details of tested RC beams

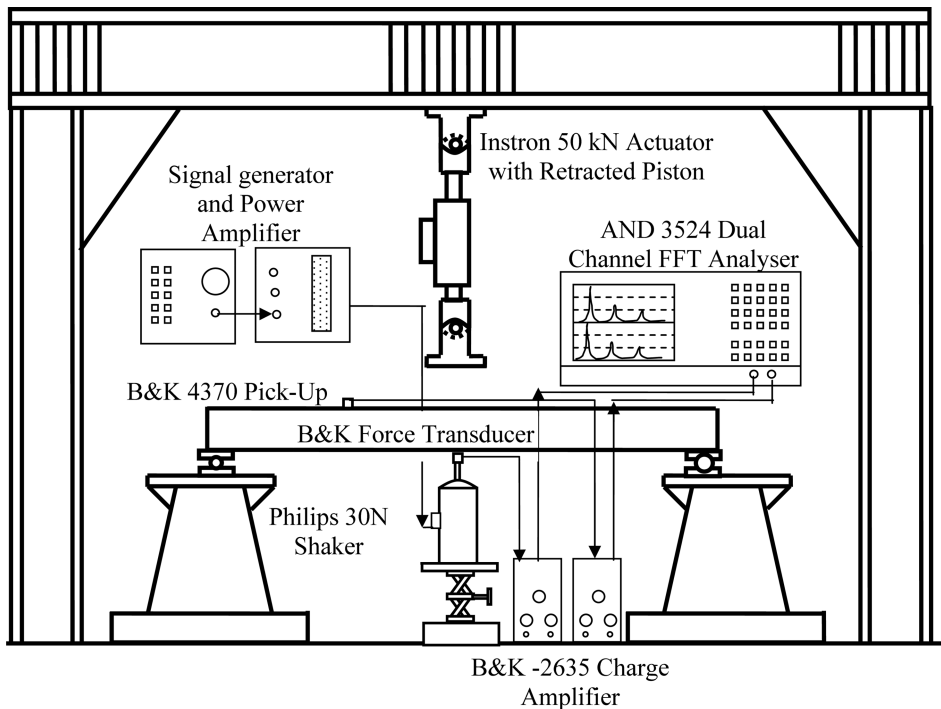


Fig. 14 Schematic view of static and dynamic testing arrangement on simply supported reinforced concrete beams

divided into two sets, one pair for symmetrical loading, with a concentrated central load and the other pair for un-symmetrical loading with an off-centric loading. Hence the induced damages are either symmetric or un-symmetric. In each pair there are two beams, one with equal reinforcement at top and bottom (2#12), type-1, UR, and the other with more number of bottom bars (4#12) and two compression-side bars (2#6), type-2, OR to tie the reinforcement cage. The concrete is designed to be M25 (Characteristic Strength of 25 MPa) and the steels are of grade Fe-415 (Yield stress of

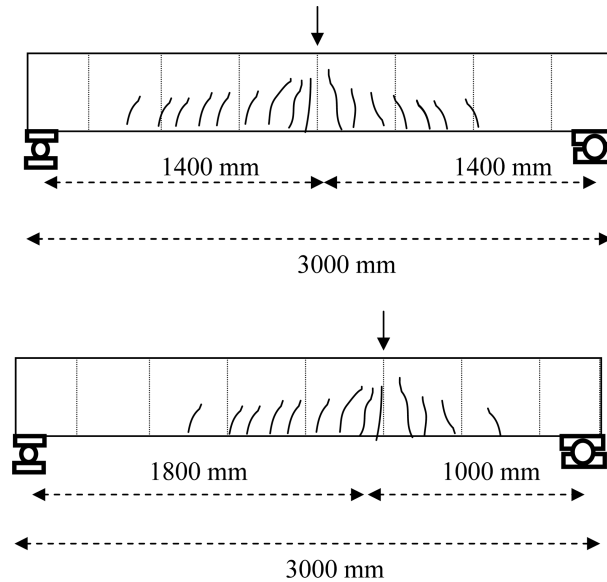


Fig. 15 Typical damage patterns in the symmetrically and un-symmetrically damaged beams

415 MPa). Fig. 13 shows the sections of the RC beam. The beams are subjected to various magnitudes of loads, starting from the virgin state to the theoretically calculated crack-initiation load, and two stages in-between the cracking and yielding stage, and a stage well beyond the yield stage (with constant load and large deflections). The applied load is measured with an in-built load cell of the Instron 50 kN servo-hydraulic actuator and the central deflection is measured with a 0.01 mm precision Mitutoyo dial gauge. After each stage of loading, the beams are un-loaded and the natural frequencies and mode shapes are measured. Fig. 14 shows the test arrangement for the dynamic measurement, which consists of a B&K-4370 accelerometer, B&K piezo-electric based force transducers, two B&K-2635 charge amplifiers for conditioning these signals and an AND dual channel FFT analyser for computing the frequency response function of the acceleration response with reference to the force input. Dynamic force is applied through a Philips 30 N electro-dynamic spring-loaded shaker, which is energised by a power amplifier with sinusoidal signal from a signal generator. Measurements are made at 29 locations each separated by 100 mm, by the rowing accelerometer. Resonances are identified by the quadrature response of (Imaginary component) FRF at different points. Fig. 15 shows the typical cracked profile of the tested beams, under symmetrical and un-symmetrical load conditions.

3. Discussion of experimental results

Table 3 gives the de-generation of the condition of the RC beams from an initial un-cracked state to various damage states, subjected to progressively increasing central concentrated loads, with reduction in flexural natural frequency as the indicator of damage. The state of damage is symmetric for both the sets of beams. The beam-type-2 (OR) by virtue of its larger reinforcement ratio has higher load capacity as evinced by its ultimate load capacity (26 kN). Various flexural

Table 3 Variation of natural frequencies for symmetrically damaged beams

Flexural Mode	Beam-Type-1 (UR) (Frequencies-Hz)					Beam-Type-2 (OR) (Frequencies-Hz)				
	Virgin State	DS1	DS2	DS3	DS4	Virgin State	DS1	DS2	DS3	DS4
Applied Load (kN)	0	2.4	7.0	14.0	14.0*	0	2.4	7.0	14.0	26.0*
1	30.00	29.125	27.575	26.325	19.33	29.50	28.38	26.83	26.13	19.83
2	108.75	108.25	106.25	99.625	79.50	107.00	106.23	103.15	102.50	90.75
3	270.00	264.00	256.75	251.95	193.85	270.00	263.0	255.40	250.56	215.63
4	422.50	417.38	404.325	389.25	332.53	425.00	417.63	403.50	399.30	345.45

Table 4 Variation of natural frequencies for un-symmetrically damaged beams

Flexural Mode	Beam-Type-1 (UR) (Frequencies-Hz)					Beam-Type-2 (OR) (Frequencies-Hz)		
	Virgin State	DS1	DS2	DS3	DS4	Virgin State	DS1	DS2
Applied Load (kN)	0	2.4	7.0	12.4	12.4*	0	7.0	26
1	30.00	29.75	28.25	28.15	24.50	30.00	29.40	25.98
2	108.50	107.75	103.27	100.00	90.00	107.00	105.40	93.85
3	270.00	269.88	258.88	256.00	229.60	269.00	268.5	239.88
4	428.00	424.00	408.00	400.83	359.30	425.00	417.13	376.30

Note : DS indicates Damage States after application of loads
 * - Load remains same but displacement is a larger value

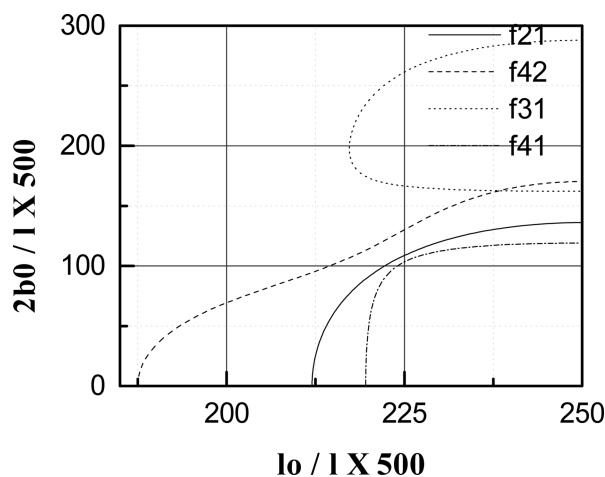


Fig. 16 Typical Iso-Eigen-Change contours for the experimental beam (Type-1, UR, DS-1)

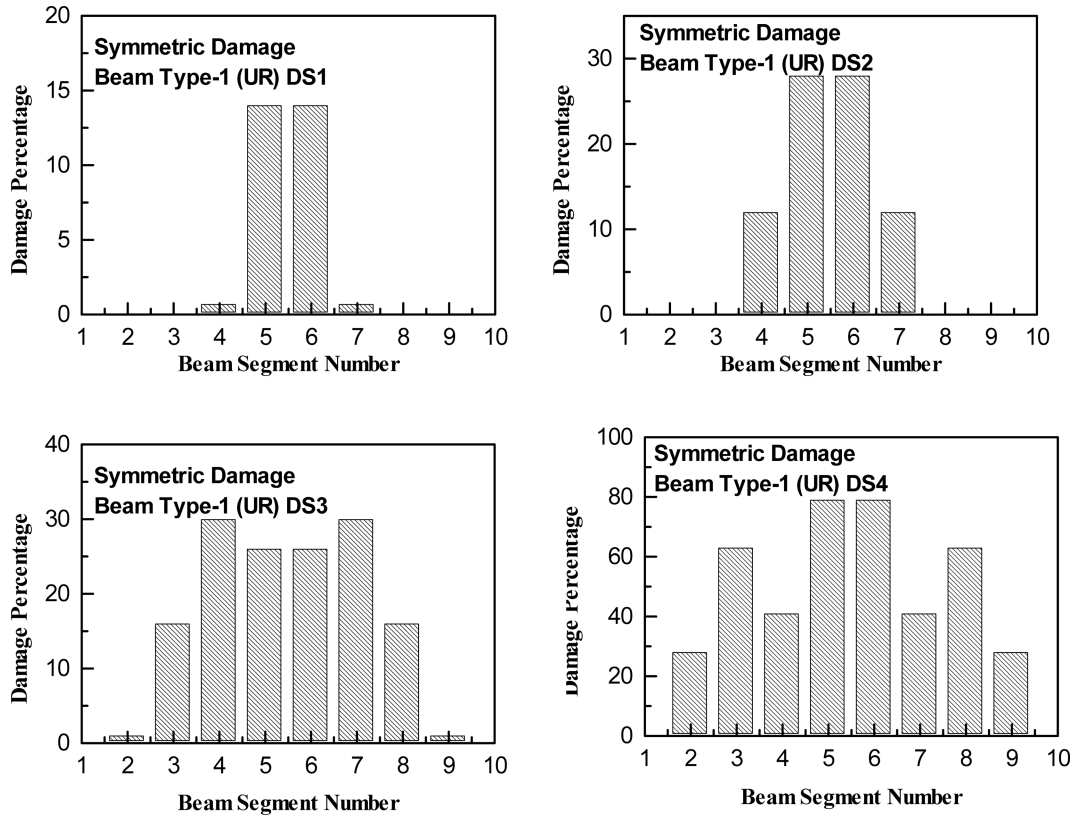


Fig. 17 Damage variation in symmetrically damaged beams (Beam Type – 1 (UR))

modes are identified by the mode shapes, which are also measured from the imaginary part of FRF. The first observation is that, applied load alone cannot be a good indicator of damage. DS3 and DS4 states, for beam-type-1 show such a big difference in frequencies for same load but for different irrecoverable energy levels. Hence the damage state as indicated by the drop in frequencies is more related with the energy lost from the system rather than the load applied. Table 4 gives the condition of the un-symmetrically damaged beams of both types under varying damage states.

For symmetrically damaged beams with a centrally located contiguous damage, the method of Iso-Eigen-Change contours is initially applied and the position of the damage is found to be at the mid-position or very close to the centre. Fig. 16 shows the identification of symmetrical damage location from Iso-Eigen-Value-Change contour. However larger scatter is seen in the curve for the extent of damage. Fig. 17 shows the retrieved damage from the frequency information, identified from the smeared damage model and using appropriate matrix equations (Eq. (16)), for beam type-1. Similar information for beam-type-2 is given in Fig. 18.

Totally ten segments of equal lengths are assumed for the smeared damage model. The end-segments are assumed to be un-damaged. A symmetrical damage assumption is made use of and the four natural frequency information is used to extract the damage in the four segments on one-side of the central-line. Both Figs. 17 and 18 show a larger damage value at the centre and as the

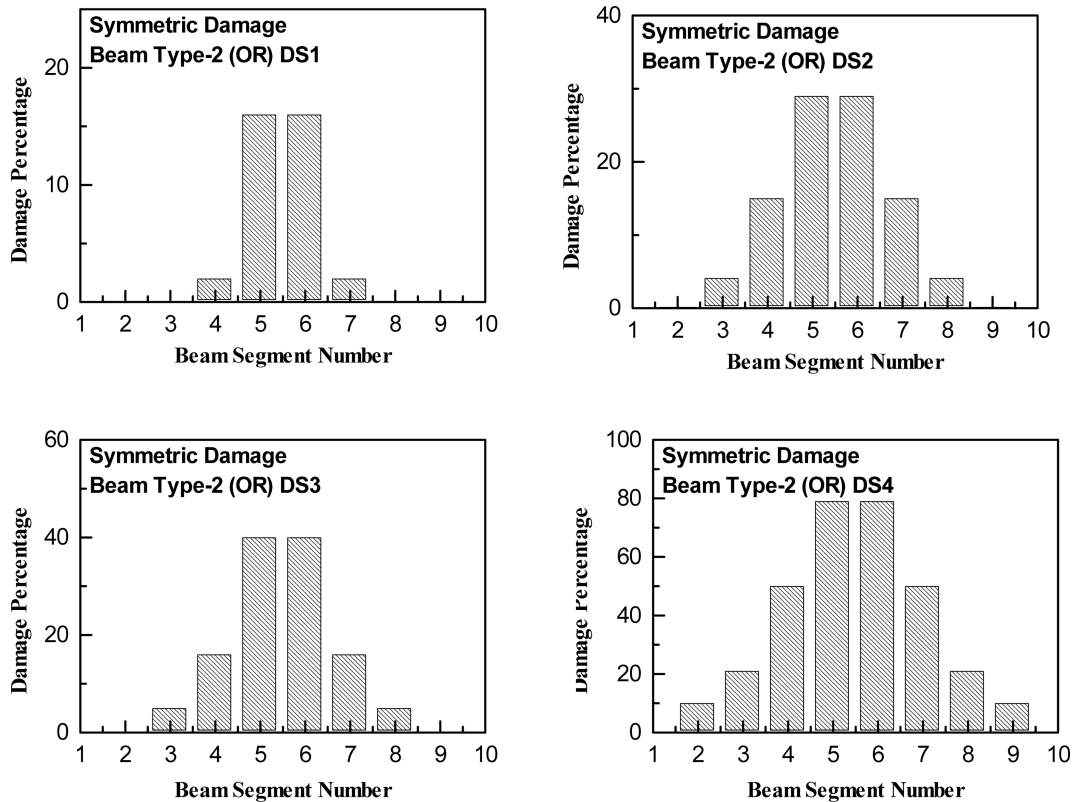


Fig. 18 Damage variation in symmetrically damaged beams (Beam Type – 2 (OR))

damage progresses, the magnitude of central damage increases and the extent of damage also increase. This can be explained as the position of the beam, where the cracking moment got just exceeded shall move farther towards the supports as the load intensity increases and hence the extent of damage should roughly correspond to these two points situated on either side of the load.

Fig. 17(c) however shows higher damage values close to mid-span but on the adjacent segments. This is little un-realistic and this shall only be attributed to the small fluctuations in the experimental results. Also, small negative damage magnitudes, predicted by this model (negative damage is growth of EI) are due to experimental fluctuations.

As discussed earlier, with a-priori information on the symmetrical nature of a contiguous, centrally located damage pattern and using Eq. (14) and Fig. 9, the extent and magnitudes of damage are retrieved for these two beam-types. For beam type-1, the damage extent $2b_0/l$ increases as 0.18, 0.30, 0.35 and 0.70, for the various damage states and the damage magnitude β increases as 0.15, 0.28, 0.36 and 0.59 respectively. For beam type-2, the damage extent $2b_0/l$ increases as 0.21, 0.30, 0.28 and 0.60, for the various damage states and the damage magnitude β increases as 0.17, 0.31, 0.41 and 0.61 respectively. Both in this case as well as in the case of Iso-Eigen-Change, the relevant expressions are derived based on a uniform damage within the damaged segment. This may not be true in the case of experimental results, where in reality a gradient of damage actually exists. Hence a deviation is likely in the prediction of the damage extent by these models, but it is surmised that the centre of damage is likely to be closer. Also, first-order perturbation method is known to falter

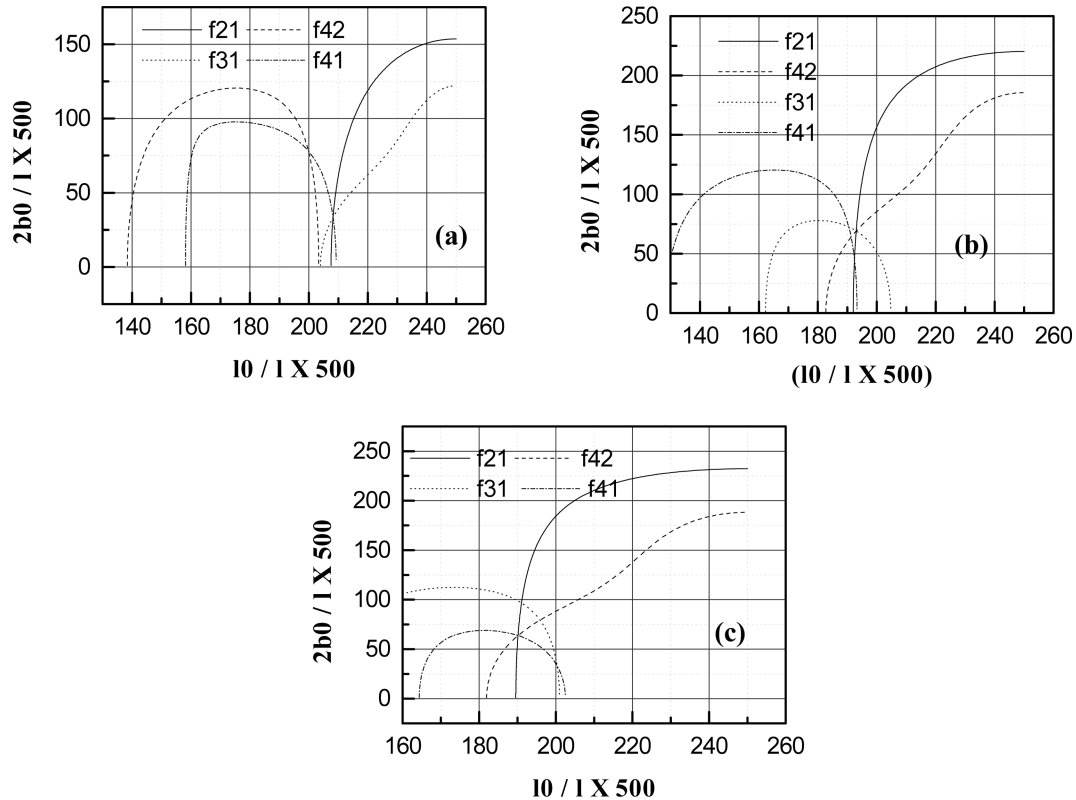


Fig. 19 Experimental damage identification using Iso-Eigen-Change contours for un-symmetrically damaged beams (a), (b) – Type-1 (UR), DS1 and DS2, (c) - Type-2 (OR), DS1

beyond a β value of 40% and prediction of 70% damage (in DS4), using smeared damage model is likely to be more erroneous. Since β cancels out in the first method, it is likely that the damage magnitudes predicted by Eq. (14) are more reliable.

Fig. 19 shows the identification of typical un-symmetrical damage location from Iso-Eigen- Value-Change contours. Though the actual damage location is 0.36ℓ , from one end of the beam, the results of the contour plot show variation ranging from 0.36 - 0.42 times ℓ . As in the symmetrical case, a scatter is seen in the extent of damage also. Having determined the position of the damage, a smeared damage model is employed in this case also and verified. For the purpose of analysis, a six-segment un-symmetrical damage distribution is assumed, with lengths of segments, 0.15 , 0.20 , 0.25 , 0.10 , 0.20 and 0.10 of ℓ . The first and last segments are assumed un-damaged and the rest of the four segments are solved using information of the four frequency changes. Fig. 20 shows the results of damage progression for beam type-1 (UR) and Fig. 21 shows the damage progression for beam type-2 (OR). As seen in the case of symmetrically damaged beams, as the applied load increases, the magnitude of damage at the load application point, (where the bending moment is also maximum) increases. Also, the extent of damage widens as the damage progresses. The negative damage is attributed to the experimental fluctuations.

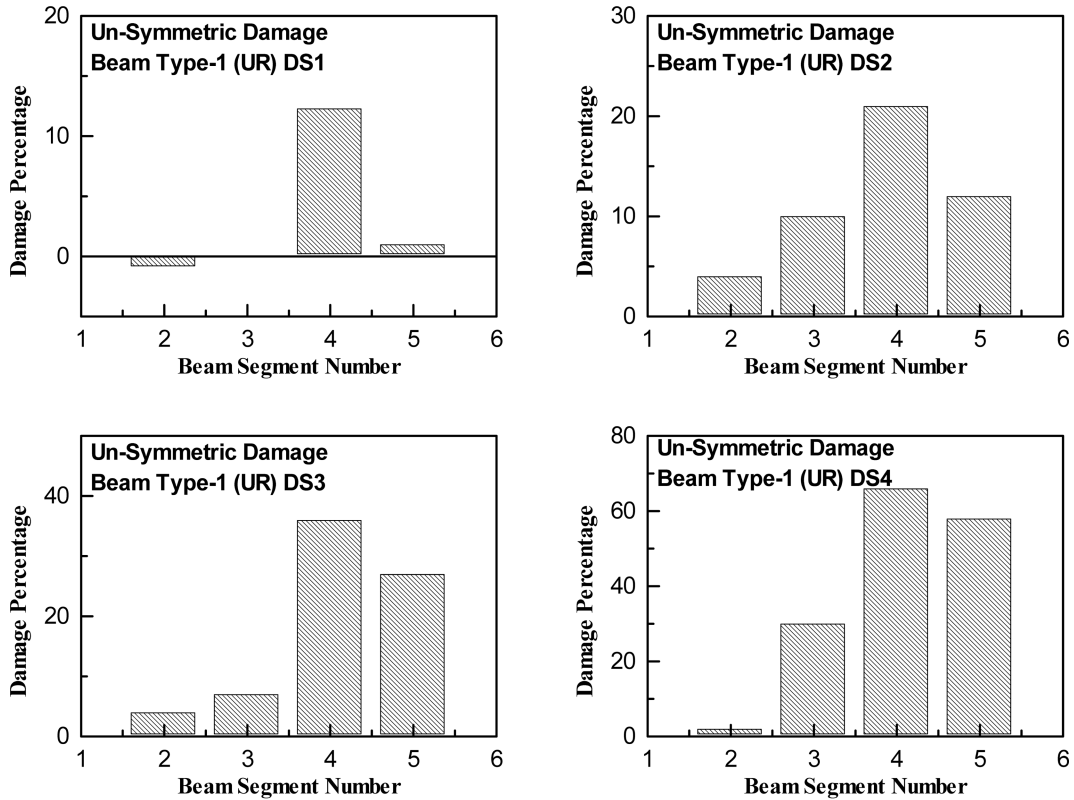


Fig. 20 Damage variation in un-symmetrically damaged beams (Beam Type – 1 (UR))

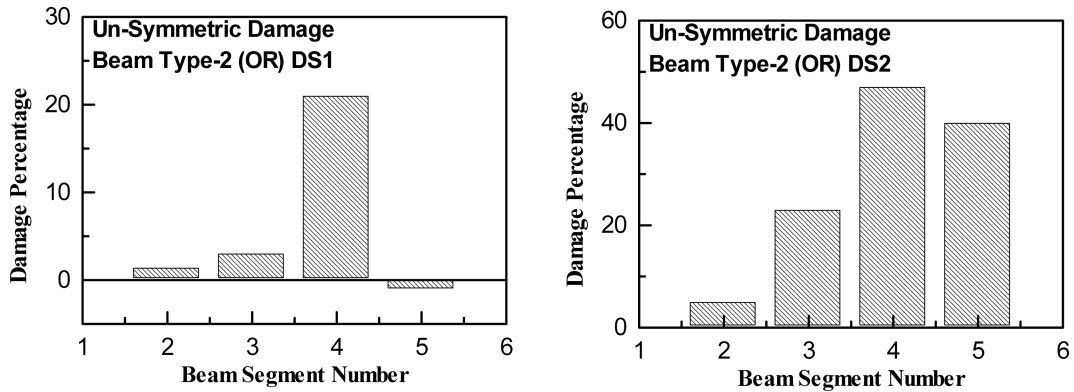


Fig. 21 Damage variation in un-symmetrically damaged beams (Beam Type – 2 (OR))

4. Conclusions

The paper compares the two models for damage estimation, one based on Iso-Eigen-Value-Change contours using the ratio of frequency change between two modes and the other based on smeared damage approach assuming a linear relationship between damage and Eigen value reduction

(smeared damage model). Both the methods are illustrated for a simply supported beam. The damage identification method using Iso-Eigen-Value-Change contours is also extended and demonstrated for a discrete five storied shear frame and the power of the method is proved. As the damage magnitude is not directly obtained by Iso-Eigen-Value-Change contours, a smeared damage identification method is to be necessarily used. This is based on first-order perturbation technique, such that damage magnitudes can also be retrieved back. Though both the methods are based on first-order perturbation technique, the cancellation of the damage magnitude in the first method indicates that it shall be more robust with reference to large change in β . For larger magnitudes of damage, the smeared damage identification method is likely to falter, however the solace is that one does not wait for a larger damage to happen, before recognising it at a smaller level. An elegant simple equation is brought out as a result of further simplification on a centrally located, symmetric, contiguous damage. The experiment conducted on a simply supported reinforced concrete beam has given encouraging results and further work is in progress in this direction for other structural elements.

Acknowledgements

The paper is published with the approval of Director, SERC. Also, the advise and encouragement of the peer reviewers in this paper and the connected previous papers have helped in re-shaping the direction of thinking of authors. Third author acknowledge the tacit guidance of Guru Ramana and the Maha Periyava of Kanchi.

References

- Casas, J.R. and Aparicio, A.C. (1994), "Structural damage identification from dynamic-test data", *J. Struct. Eng.-ASCE*, **120**, 2437-2450.
- Cawley, P. and Adams, R.D. (1979), "The location of defects in structures from measurements of natural frequencies", *J. Strain Anal. Eng.*, **14**, 49-57.
- Cerri, M.N. and Vestroni, F. (2000), "Detection of damage in beams subjected to diffused cracking", *J. Sound Vib.*, **234**, 259-276.
- Cerri, M.N. and Vestroni, F. (2005), "Use of frequency change for damage identification in reinforced concrete beams", *J. Vib. Control*, **9**, 475-491.
- Choudhury, M.R. and Ramirez, M. (1992), "A comparison of the modal responses for a defective versus non-defective concrete test beams", *Proceedings of the Tenth International Modal Analysis Conference*, San Diego, CA.
- Dilena, M. and Morassi, A. (2004), "The use of anti-resonances for crack detection in beams", *J. Sound Vib.*, **276**, 195-214.
- Dilena, M. and Morassi, A. (2009), "Structural health monitoring of rods based on natural frequency and anti-resonant frequency measurements", *Struct. Health Monit.*, **8**, 149-173.
- Doebling, S.W., Farrar, C.R., Prime, M.B. and Shevitz, P.W. (1996), "Damage Identification. Health monitoring of structural and mechanical systems from changes in their vibration characteristics – A literature review", Los Alamos National Laboratory, Los Alamos, New Mexico.
- Gatti, P.L. and Ferrari, V. (1999), *Applied Structural and Mechanical Vibrations, Theory, Methods and Measuring Instrumentations*, E&F.N Spon, London.
- Gladwell, G.M.L. (2004), *Inverse Problems in Vibration Second Ed.*, Kluwer Academic Publishers, Dordrecht.
- Hassiotis, S. and Jeong, G.D. (1993), "Assessment of structural damage from natural frequency measurements",

- Comput. Struct.*, **49**(4), 679-691.
- Hassiotis, S. (2000), "Identification of damage using natural frequencies and Markov parameters", *Comput. Struct.*, **74**, 365-373.
- Ju, F. and Mimovich, M. (1986), "Modal frequency method in diagnosis of fracture damage in structures", *Proceeding of the Fourth International Modal Analysis Conference*, Los Angeles, CA.
- Lakshmanan, N., Srinivasulu, P. and Parameswaran, V.S. (1991), "Post cracking stiffness and damping in reinforced concrete beam elements", *J. Struct. Eng.*, India, **17**(4), 1405-1411.
- Lakshmanan, N., Raghuprasad, B.K., Muthumani, K., Gopalakrishnan, N. and Basu, D. (2007a), "Wavelet analysis and enhanced damage indicators", *Smart Struct. Syst.*, **3**, 23-49.
- Lakshmanan, N., Raghuprasad, B.K., Muthumani, K., Gopalakrishnan, N. and Sreekala, R. (2007b), "Seismic damage estimation through measurable dynamic characteristics", *Comput. Concrete*, **4**, 167-186.
- Lakshmanan, N., Raghuprasad, B.K., Muthumani, K., Gopalakrishnan, N. and Basu, D. (2008a), "Damage evaluation through radial basis function network (RBFN) based artificial neural network scheme", *Smart Struct. Syst.*, **4**, 23-49.
- Lakshmanan, N., Raghuprasad, B.K., Muthumani, K., Gopalakrishnan, N. and Basu D. (2008b), "Identification of reinforced concrete beam-like structures subjected to distribute damage from experimental static measurements", *Comput. Concrete*, **5**, 70-90.
- Lakshmanan, N., Raghuprasad, B.K., Gopalakrishnan, N., Sathishkumar, K. and Murthy, S.G.N. (2010), "Detection of contiguous and distributed damage through contours of equal frequency change", *J. Sound Vib.*, **329**, 1310-1331.
- Liang, R.Y., Hu, J. and Choy, F. (1992), "Theoretical study of crack induced Eigen frequency changes on beam structures", *J. Eng. Mech.-ASCE*, **118**, 384-396.
- Morassi, A. (2001), "Identification of a crack in a rod based on changes in a pair of natural frequencies", *J. Sound Vib.*, **242**, 577-596.
- Morassi, A. (2007), "Damage detection and generalized Fourier coefficients", *J. Sound Vib.*, **302**, 229-259.
- Nandwana, B.P. and Maiti, S.K. (1997), "Detection of location and size of a crack in stepped cantilever beams based on measurement of natural frequencies", *J. Sound Vib.*, **203**, 435-446.
- Neild, S.A., Williams, M.S. and McFadden, P.D. (2003), "Non-linear vibration characteristics of damaged concrete beams", *J. Struct. Eng.-ASCE*, **129**, 26-268.
- Patil, D.P. and Maiti, S.K. (2003), "Detection of multiple cracks using frequency measurements", *Eng. Fract. Mech.*, **70**, 1553-1572.
- Owolabi, G.M., Swamidas, A.S.J. and Seshadri, R. (2003), "Crack detection in beams using changes in frequencies and amplitudes of frequency response functions", *J. Sound Vib.*, **265**, 1-22.
- Palacz, M. and Krawczuk, M. (2002), "Vibration parameters for damage detection in structures", *J. Sound Vib.*, **249**, 999-1010.
- Prime, M.B. and Shevitz, D.W. (1996), "Linear and non-linear methods for detecting cracks in beams", *Proceeding of 14th International Modal Analysis Conference*, Honolulu.
- Rajagopalan, N., Lakshmanan, N. and Muthumani, K. (1996), "Stiffness degradation of reinforced concrete beams under repeated low energy impact loading", *Indian Concrete J.*, **69**(4), 227-234.
- Rajagopalan, N., Lakshmanan, N. and Jeyasehar, C.A. (1999), "Damage assessment in reinforced concrete beams using natural frequencies", *J. Struct. Eng.*, India, **26**(3), 165-172.
- Silva, J.M.M. and Gomes, A.J.M.A. (1994), "Experimental dynamic analysis of cracked free-free beams", *J. Exp. Mech.*, **30**(1), 20-25.
- Yang, X.F., Swamidas, A.S.J. and Seshadri, R. (2001), "Crack identification in vibrating beams using the energy-based method", *J. Sound Vib.*, **244**(2), 339-357.